

# Sheaf Discovery with Joint Computation Graph Pruning and Flexible Granularity

Lei Yu<sup>1\*</sup>, Jingcheng Niu<sup>12\*</sup>, Zining Zhu<sup>13</sup>, Xi Chen<sup>1</sup>, Gerald Penn<sup>1</sup>

<sup>1</sup>University of Toronto, <sup>2</sup>UKP Lab, TU Darmstadt, <sup>3</sup>Stevens Institute of Technology

## Abstract

In this paper, we introduce DiscoGP, a novel framework for extracting self-contained modular units, or *sheaves*, within neural language models (LMs). Sheaves extend the concept of functional *circuits*, a unit widely explored in interpretability research, by considering not only subsets of edges in an LM’s computation graph but also the model’s weight parameters. Our framework identifies sheaves through a gradient-based pruning algorithm that operates on both of these in such a way that reduces the original LM to a sparse skeleton that preserves certain core capabilities. Experimental results demonstrate that, across a range of linguistic and reasoning tasks, DiscoGP extracts sheaves that preserve 93-100% of a model’s performance on the identified task while comprising only 1-7% of the original weights and connections. Furthermore, our analysis reveals that, compared to previously identified LM circuits, the sheaves discovered by DiscoGP exhibit superior modularity and functional fidelity. Extending our method to the neuron level also unveils novel insights into the inner workings of LLMs.<sup>1</sup>

## 1 Introduction

Systems built with transformer language models (LMs; Vaswani et al., 2017; Devlin et al., 2019; Radford et al., 2019; Raffel et al., 2020; OpenAI, 2023; Touvron et al., 2023) have demonstrated incredible capabilities in solving various natural language tasks across different fields. The exact mechanisms by which these models achieve these results remain poorly understood, however. Researchers in the field of interpretability therefore aim to provide human-understandable explanations of the computational mechanisms of these “black-boxed” LMs.

\*Equal contribution.

<sup>1</sup>The code and results of DiscoGP are available online: [https://github.com/frankniujc/disco\\_gp](https://github.com/frankniujc/disco_gp).

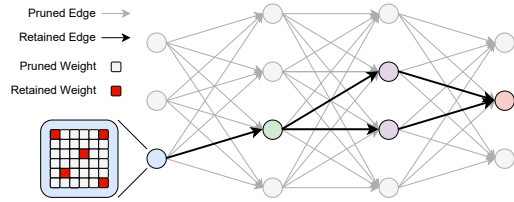


Figure 1: Illustration of DiscoGP. By combining computation-edge and weight-parameter pruning, DiscoGP achieves better performance with neuron-level granularity.

Should one of these interpretations become available, it could lead to the improvement of LMs with better controllability and performance, and even germinate a subsequent generation of explainable artificial intelligence (XAI) systems.

Now, a nascent “circuit”-based framework has emerged that aims to explain this process and provide the most convincing explanation of LM behaviours to date. This generally decomposes the computation process of an LM into a directed acyclic graph (DAG) and identifies a subset of model components and connections (information flow) that correspond to specific model behaviours. Initially, these circuits were identified manually using various activation or attention patching methods (Wang et al., 2022). ACDC (Conmy et al., 2023) automated the circuit-discovery process. Since then, several follow-up attempts (Syed et al., 2024; Hanna et al., 2024; Zhang et al., 2025) have been proposed to further advance the state-of-the-art in circuit discovery.

The term *circuit*, however, is used to refer to several distinct concepts, even within the LM interpretability community. We provide a survey of the nomenclature (§2) and clarify our own intentions in respect of interpretation. With a thorough and rigorous definition of the computation graph, edge pruning, and weight pruning, we introduce *sheaf* as a new technical term: a subset of edges in the

computation graph and weights in the model that, when executed in isolation, can preserve the original model’s behaviour or capabilities on a given task. Simply put, we seek to identify the interpretable sheaf of model components within the LM “haystack.”

Sheaf discovery fills a gap in current mechanistic interpretability research in that it identifies a self-contained collection of model units that can perform a particular LM function in isolation. Whereas recent attempts have boasted of their performance on the basis of *post hoc* dissections revealing that the discovered circuit was of crucial importance, our own perspective is that, for all but the most esoteric of purposes, circuits are not worth discovering if they cannot operate by themselves. For this reason, we follow the regimen of “zero ablation,” in which layer heads not identified during training as part of a sheaf are zeroed out during evaluation. Until now, although zero ablation is occasionally acknowledged as a worthwhile goal, this has not been standard practice. Sheaves offer a unique opportunity to manipulate self-contained units and gain novel insights into the internal workings of transformer-based LMs.

Prior automatic circuit-discovery methods share a crucial limitation, moreover: the computational power they require is prohibitively large because the number of edges in the computation graph grows quadratically ( $O(n^2)$ ) with the number of model components. This has prevented researchers from engaging in discovery at the neuronal level. The presence of a parallel thread of investigation into the properties of MLP neurons, finding them to be highly idiosyncratic in both the type of information they contain and their function within large neural networks (Geva et al., 2021; Dai et al., 2022; Meng et al., 2022; Niu et al., 2024; Hong et al., 2024), however, does suggest that refining the granularity of these interpretations to the neuronal level would be valuable. Recent work on the “knowledge neuron thesis” (Niu et al., 2024; Dai et al., 2022), for example, has shown that modifying just a few neurons, or even a single neuron, can lead to substantial changes in the model’s behaviour.

The **Discovery with Joint Computation Graph Pruning** (DiscoGP) framework addresses the granularity and scaling problem by applying joint computation-edge and model-weight parameter pruning with gradient-based masking. While the computation graph is still defined at the relatively coarse level of attention heads and MLPs, as in

other circuit-discovery methods, DiscoGP extends this approach to weight pruning within each individual computation-graph node to enable finer, neuron-level discovery.

DiscoGP achieves state-of-the-art performance in sheaf detection: it identifies the sheaves for a wide range of tasks with the fewest edges and weight parameters while maintaining near-perfect performance compared to the original model’s performance. By refining granularity to the neuronal level, we unveil several critical insights into the model that were previously unavailable.

We begin with a formal definition of **sheaves**, and provide a survey that clarifies the various different uses of the term *circuit* in relevant literature (§2). Then, we introduce **DiscoGP**, a novel sheaf-discovery framework with joint pruning of weight parameters and computation-graph edges that enables individual neuron-level granularity (§3). Using DiscoGP, we can obtain sheaves across a wide range of tasks that are **sparser and yet more faithful** to the original model.

## 2 Sheaves and Circuits

In this section, we present a comprehensive definition of the main task of *sheaf discovery*, and discuss its similarities and differences compared to the broad range of tasks often referred to as “circuit discovery” in the literature, as the term is used inconsistently and can sometimes cause confusion. We start with a survey of the different definitions of circuit discovery (§2.1), and then introduce our sheaf-based framework by defining weight pruning (§2.2) and edge pruning (§2.3).

### 2.1 Survey: Circuits and Circuit Discovery

**Circuit** The term “circuit” has various meanings within the LM interpretability community, depending on the context. Nanda (2022) describes it as “a fairly fuzzy and poorly defined term” that roughly refers to “the sub part [sic] of a model that does some understandable computation to produce some interpretable features from prior interpretable features.” Olah et al. (2020) considered circuits as a set of features and the weighted connections between them. Elhage et al. (2021) used the term “circuit” to refer to the separable parts of the computation process within each attention head. Because the computation of a transformer model can generally be considered linear, Elhage et al. (2021) argued that the computation of the query and key

matrices and the output and value matrices can be considered as two largely independent QK and OV circuits. More recently, work in the field typically decomposes an LM into functional “building blocks” and considers the collection of these blocks and a subset of their connections as a circuit; but what constitutes building blocks may still differ from paper to paper. Wang et al. (2022) referred to a circuit as the collection of attention heads, while ACDC used the term “circuit” to refer to the subset of edges between attention heads and MLPs in the computation graph.

**Circuit Discovery** The task of identifying the aforementioned circuits in pre-trained transformer LMs is called *circuit discovery*. Early studies typically searched for circuits manually during simple tasks such as rudimentary anaphora resolution (Wang et al., 2022) or simple arithmetic reasoning (Hanna et al., 2023), using a combination of interpretability tools, including causal interventions (Vig et al., 2020; Meng et al., 2022) and logit lenses (Geva et al., 2022, 2023; Yu et al., 2024a). More recently, ACDC (Conmy et al., 2023) automated the circuit-discovery process. Specifically, they used the activation-patching technique (Goldowsky-Dill et al., 2023; Zhang and Nanda, 2023), or its approximations (Nanda, 2023), to assess a computation edge’s importance by first knocking it out and observing its effect on the model’s final output. Beginning at the output node and proceeding in reverse topological order, they evaluate the effect of removing each of the node’s incoming edges individually. If the removal of an edge has a greater effect than a predetermined threshold, the edge is included in the circuit; otherwise, it is pruned. Syed et al. (2024) extended ACDC with attribution patching to achieve improved results.

Recent work has also explored other notions of circuithood, such as formulating circuits as collections of human-interpretable neural activation features (Huben et al., 2024; Marks et al., 2024; Yu et al., 2024b), collections of attention heads (Niu et al., 2025), or as distributed neural representations of proposed symbolic algorithms (Geiger et al., 2021; Wu et al., 2023).

Most automated circuit-discovery studies evaluate their methods based on their structural overlap with previously discovered or manually hardwired circuits (Conmy et al., 2023; Syed et al., 2024). We concur with recent critiques of this evaluation metric (Hanna et al., 2024), and note that the functional

fidelity (often quaintly termed functional *faithfulness*) metric, measuring how well the circuit reproduces the original model’s performance, is a more appropriate criterion for this task.

## 2.2 Weight Pruning

Weight pruning is a technique widely used in the model interpretability community to identify subnetworks (a subset of a model’s weight parameters) associated with specific functions of a neural network (Cao et al., 2021; Csordás et al., 2021; Zhang et al., 2021; Guo et al., 2021; De Cao et al., 2022). More recently, Lepori et al. (2023) extended this work to transformer-based language models. Figure 2a provides an overview of weight pruning. This line of research has been encouraged in part by Frankle and Carbin’s (2019) Lottery Ticket Hypothesis, which states that it is possible to identify smaller functional subnetworks even within dense, randomly initialized models. When this subnetwork is trained from scratch with a similar computational budget, it can achieve performance comparable to that of the original model. Using the *continuous sparsification* method (Figure 2a), Savarese et al. (2020) demonstrated that this subnetwork can be directly extracted from a neural network that maintains task performance without the need for retraining, as originally suggested in the hypothesis. The method is also sometimes referred to as *differentiable masking* (De Cao et al., 2022). It is not always — there are many ways to approximate a gradient without using analytic differentiation.

## 2.3 Computation Graph and Edge Pruning

**Computation Graph** Elhage et al. (2021) introduced the concept of a *residual stream*, providing a clear and concise view of the computation within a transformer block. Each block consists of an attention module followed by an MLP module. Encoder blocks are stacked like layers of a neural network, but they have many layers inside them. Let  $x_i$  be the input to the  $i$ -th transformer block, with  $H^{(i)}$  representing the set of attention heads and  $f_i$  denoting the MLP module, we can write the output of the  $i$ -th block ( $x_{i+1}$ ) in a transformer as:

$$x_{i+1} = \overbrace{x_i + \sum_{h \in H^{(i)}} h(x_i) + f_i(x_i^{\text{mid}})}^{\text{x}_i^{\text{mid}}}. \quad (1)$$

To demonstrate the concept of a computation graph, let us consider a simple one-block transformer

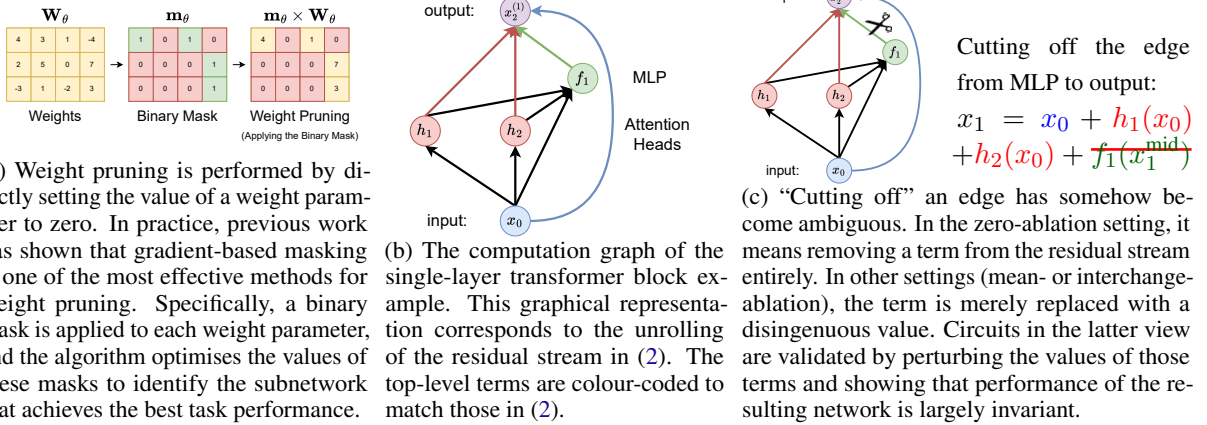


Figure 2: Illustration of the formulation of sheaf discovery: computation graph, weight pruning and edge pruning.

model with the input embedding  $x_0$ . We can “unroll” the residual stream (Nanda and Bloom, 2022) as shown in (2). From this stream, we can tell that the final output of this small transformer consists of 4 terms: the original word embedding input  $x_0$ , the output of the two attention heads  $h_1(x_0)$  and  $h_2(x_0)$ , as well as the output of the MLP module  $f_1(x_0 + h_1(x_0) + h_2(x_0))$ .

$$\begin{aligned} x_1^{\text{mid}} &= x_0 + h_1(x_0) + h_2(x_0) \\ x_1 &= x_1^{\text{mid}} + f_1(x_1^{\text{mid}}) = x_0 + \textcolor{red}{h_1(x_0)} + \textcolor{red}{h_2(x_0)} + f_1(x_0 + h_1(x_0) + h_2(x_0)). \end{aligned} \quad (2)$$

From the unrolled residual stream, we can understand how information flows within the transformer block. Using (2) as an example, the output  $(x_2)$  is derived from the outputs of the two attention heads  $(h_1, h_2)$ , the MLP  $(f_1)$  output, and the original input embedding  $(x_0)$ . The attention heads only take  $x_0$  as input, while  $f_1$  receives both the outputs of the attention heads and  $x_0$ . Based on this information flow, we can construct a computation graph as shown in Figure 2b.

**Edge Pruning** The introduction of computation graphs allows us to analyse the impact of information flow between model components. Examining how pruning<sup>2</sup> a computation edge in this graph affects the model’s final output reveals the importance of that specific information flow. In DiscoGP, as shown in Figure 2c, the pruning of an edge is equivalent to the removal of a term in the unrolled residual stream, which can be achieved either through greedily applying causal mediation methods (Vig et al., 2020; Finlayson et al., 2021; Meng et al., 2022) to identify important edges (Conmy

et al., 2023), or by leveraging gradient-based techniques to mask out non-essential component connections (Bhaskar et al., 2024).

### 3 DiscoGP: Sheaf Discovery

Weight pruning and circuit pruning are not mutually exclusive, so why not apply both? Here, we introduce the term “sheaf” to describe the intersection of our particular brand of circuit pruning (edge pruning) and subnetwork pruning (weight pruning). Let  $G = \{E, V\}$  represent the computation graph, and let  $\Theta$  denote the set of all parameters of the model. The task of identifying a sheaf involves searching for two binary masks,  $\mathbf{m} = (\mathbf{m}_\theta, \mathbf{m}_E) \in \{0, 1\}^{|\theta|+|E|}$ , which correspond to the pruned weights and edges, respectively. Similar to prior weight pruning approaches, DiscoGP uses Gumbel sigmoid distributions in both masks, enabling the search for a globally optimal solution across weight and edge pruning. This section outlines the sheaf-discovery procedure and the DiscoGP joint pruning algorithm.

In summary, sheaf discovery has three steps:

1. For an LM capability, define a task corresponding to the capability by constructing a dataset;
2. Search for a sheaf (a collection of edges and weight parameters) corresponding to the dataset;
3. Evaluate the functional fidelity of the sheaf – i.e., determine whether the model can still perform the task after turning off all other components that do not belong to the sheaf.

These three steps of sheaf discovery bear some superficial resemblance to the three steps of the “automatic circuit-discovery workflow” proposed by Conmy et al. (2023). They argue that researchers

<sup>2</sup>Also referred to as *knockout*, *cut-off*, or *ablation*.

Dataset	Example Prompt	Correct	Incorrect
BLiMP	Raymond is selling this __	sketch	sketches
IOI	When Mary and John went to the store, John gave a drink to __   Mary   John		
OQA	The capital city of Canada is __   Ottawa   *not unique		

Table 1: An overview of the tasks and datasets.

should “perform an extensive and iterative series of patching experiments with the goal of removing as many unnecessary components and connections from the model as possible” (Conmy et al., 2023). Our framework differs in two key respects: (1) we do not impose any restrictions on patching-based approaches; and (2) we aim to identify sheaves of high functional fidelity — in other words, while ACDC’s goal is to identify the most salient components and edges, it does not guarantee that the resulting “circuits” can perform the task by itself.

### 3.1 Joint Weight and Edge Pruning

Similar to previous work on gradient-based mask learning (Louizos et al., 2018; Csordás et al., 2021; Cao et al., 2021; De Cao et al., 2022; Bayazit et al., 2023), DiscoGP models each mask  $m_i \in \mathbf{m}$  as a random variable, parameterised by a hard-concrete or gumbel-sigmoid distribution. We first compute a continuous score  $s_i \in [0, 1]$ :

$$s_i = \sigma\left(\frac{l_i - \log \frac{\log \mathcal{U}_1}{\log \mathcal{U}_2}}{\tau}\right), \quad (3)$$

where  $\tau \in (0, \inf)$  is a temperature hyperparameter,  $l_i$  is a learnable logit parameter of a sigmoid distribution  $\sigma(\cdot)$ , and  $\mathcal{U}_1, \mathcal{U}_2 \sim \text{Uniform}(0, 1)$  are random variables drawn from a uniform distribution. We then use the straight-through estimator (Bengio et al., 2013) to convert the sampled  $s_i$  into a binary mask variable:

$$m_i = [\mathbb{1}_{s_i > 0.5} - s_i]_{\text{detach}} + s_i, \quad (4)$$

where  $\mathbb{1}$  represents the indicator function, and  $[\cdot]_{\text{detach}}$  is an operator that blocks gradient flow during backpropagation. This approach makes the binary mask  $m_i$  a differentiable function of the logit  $l_i$ , allowing it to be optimised through backpropagation for specific objectives.

**Sheaf Searching Objectives** Given a task dataset  $\mathcal{D} = \{\mathbf{x}, \hat{\mathbf{y}}\}$ , where  $\mathbf{x}$  represents the input and  $\hat{\mathbf{y}}$  is the output of the original model, our aim is to identify a set of masks  $\mathbf{m}$  on weights and edges, such that the pruned sheaf produces results as close

to the original model as possible. To achieve this, we define **functional fidelity loss** as the negative log-likelihood of the original model’s predicted label in the output distribution of the pruned circuit:

$$\mathcal{L}_{\text{fidelity}} = -\sum_i \log p_{\mathbf{m}}(\hat{y}_i | x_i). \quad (5)$$

Moreover, we want the sheaf to contain as many function-specific weights and edges as possible. In other words, when the detected sheaf is removed from the original model, the remaining computational graph should perform at near-random levels on  $D$ . Let  $\tilde{\mathbf{m}} = 1 - \mathbf{m}$  denote the reverse mask of  $\mathbf{m}$ , and the **complementary sheaf** be the sheaf induced by the reverse mask of  $\mathbf{m}$ . We define the **completeness loss** as the cross-entropy between the output distribution of the complementary sheaf and a uniform distribution over the label space  $\{y_k\}_{k=1}^K$ :

$$\mathcal{L}_{\text{complete}} = -\sum_i \sum_{k=1}^K \frac{1}{K} \log p_{\tilde{\mathbf{m}}}(y_k | x_i). \quad (6)$$

Lastly, we want the sheaf to be as sparse as possible. Therefore, we minimize the **sparsity loss**:

$$\begin{aligned} \mathcal{L}_{\text{sparse}} &= \mathcal{L}_{\text{sparse}/\theta} + \mathcal{L}_{\text{sparse}/E} \\ &= \frac{1}{|\mathbf{m}_\theta|} \sum_{i=1}^{|\mathbf{m}_\theta|} \sigma(l_i) + \frac{1}{|\mathbf{m}_E|} \sum_{i=1}^{|\mathbf{m}_E|} \sigma(l_i). \end{aligned} \quad (7)$$

The final objective function is then comprised of a weighted mixture of the three loss terms:

$$\mathcal{L}_{\text{GP}} = \mathcal{L}_{\text{fidelity}} + \lambda_c \mathcal{L}_{\text{complete}} + \lambda_s \mathcal{L}_{\text{sparse}}, \quad (8)$$

where  $\lambda_c, \lambda_s$  are hyperparameters that regulate relative loss importance.

**DiscoGP Implementation Details** Due to page limitations, other optimisation techniques we implemented, including *post hoc* sheaf pruning and split QKV pruning, are treated in Appendix A.

Task	Discovery Method	Sheaf Acc. (%) (higher is better)	KL Div. (lower is better)	Comp. Acc. (%) (random* is better)	Weight Density (%) (lower is better)	Edge Density (%) (lower is better)
anaphor gender agr. (AGA)	ACDC	83.3	0.121	42.7	100	6.48
	EAP	89.3	0.091	53.9	100	4.88
	Edge Pruning	88.4	0.137	49.7	100	6.62
	Weight Pruning	97.1	0.078	50.2	3.01	100
	DiscoGP (Ours)	<b>98.5</b>	<b>0.074</b>	49.9	<b>1.58</b>	<b>3.88</b>
anaphor number agr. (ANA)	ACDC	81.0	0.250	67.0	100	6.26
	EAP	95.3	0.049	56.3	100	8.66
	Edge Pruning	87.9	0.178	39.3	100	2.78
	Weight Pruning	97.7	0.076	40.3	2.79	100
	DiscoGP (Ours)	<b>99.7</b>	<b>0.043</b>	39.2	<b>1.36</b>	<b>1.94</b>
det. noun agr. 1 (DNA)	ACDC	85.3	0.129	46.3	100	7.35
	EAP	85.7	0.138	40.6	100	9.83
	Edge Pruning	83.7	0.114	59.3	100	2.27
	Weight Pruning	95.3	0.099	53.0	0.280	100
	DiscoGP (Ours)	<b>95.3</b>	<b>0.098</b>	51.7	<b>0.187</b>	<b>1.92</b>
det. noun irr. 1 (DNA i)	ACDC	62.7	0.419	39.3	100	6.61
	EAP	60.0	0.434	38.3	100	8.92
	Edge Pruning	67.1	0.374	48.0	100	2.46
	Weight Pruning	94.3	0.103	53.6	0.263	100
	DiscoGP (Ours)	<b>95.8</b>	<b>0.102</b>	47.2	<b>0.244</b>	<b>1.68</b>
det. noun adj. 1 (DNA a)	ACDC	82.4	0.169	52.3	100	7.04
	EAP	83.5	0.153	45.7	100	9.90
	Edge Pruning	50.3	0.412	47.6	100	7.14
	Weight Pruning	94.7	0.136	49.9	0.565	100
	DiscoGP (Ours)	<b>95.5</b>	<b>0.118</b>	45.3	<b>0.520</b>	<b>5.71</b>
det. noun adj. irr. 1 (DNA ia)	ACDC	50.2	0.120	41.4	100	9.46
	EAP	60.7	0.128	44.7	100	6.89
	Edge Pruning	56.3	0.348	47.8	100	12.9
	Weight Pruning	94.6	0.127	49.9	0.569	100
	DiscoGP (Ours)	<b>95.1</b>	<b>0.118</b>	45.3	<b>0.496</b>	<b>6.22</b>
IOI	ACDC	51.6	0.730	50.6	100	2.45
	EAP	58.3	0.756	55.2	100	3.48
	Edge Pruning	100	0.032	49.9	100	2.97
	Weight Pruning	98.4	0.043	57.5	1.87	100
	DiscoGP (Ours)	<b>100</b>	<b>0.020</b>	49.2	<b>1.79</b>	<b>2.03</b>
PARAREL Average <sup>†</sup>	ACDC	1.0	0.379	0.6	100	5.35
	EAP	0.9	0.341	0.6	100	5.92
	Edge Pruning	90.4	0.039	0.7	100	2.97
	Weight Pruning	91.8	0.032	0.8	2.83	100
	DiscoGP (Ours)	<b>93.1</b>	<b>0.023</b>	0.62	<b>2.77</b>	<b>2.91</b>

Table 2: Sheaf-Discovery Performance Comparison. DiscoGP achieves the best performance across all tasks, using the fewest weight parameters and edges. The best-performing methods are highlighted in **bold**. \*: For complement sheaf accuracy, successful searches are expected to yield random performance. Scores close to random therefore indicate good performance, although a direct comparison of complement scores would not be meaningful. BLiMP and IOI’s expected random performance is 50%, and PARAREL’s expected random performance is close to 0%. <sup>†</sup>: Due to page limits, only the average training set performance is shown. Full PARAREL results are provided in Appendix D and support the same findings.

## 4 Experimental Setup

**Evaluation:** We evaluate DiscoGP and the baselines across three tasks (Table 1): syntactic agreement from the **BLiMP** corpus (Warstadt et al., 2020), the indirect object identification (**IOI**) task introduced by Wang et al. (2022), and factual information from open-domain question answering (**OQA**) with the **PARAREL** (Elazar et al., 2021)

dataset. This ensemble of tasks is intended to provide comprehensive coverage of syntactic, semantic and factual aspects. See Appendix B for more information.

Metric-wise, we report the **functional fidelity**: this includes the sheaf’s accuracy and the KL divergence of the sheaf’s output (sheaf accuracy refers to the task accuracy when all pruned components are zero-ablated and sheaf KL divergence is mea-

sured between the sheaf’s output and that of the original model). We also report completeness or the **complement sheaf accuracy** (i.e., the accuracy when the sheaf is zero-ablated and all other model components are kept on), as well as **sparsity** (both edge and weight sparsity). These evaluation metrics follow the typical fidelity, completeness and sparsity scheme used by other mechanistic interpretability work (Wang et al., 2022; Conmy et al., 2023; Syed et al., 2024; Bhaskar et al., 2024).

**Baseline Methods:** We compare DiscoGP with every other major circuit-discovery method. We categorize the methods into (1) threshold-based greedy search algorithms, which include ACDC (Conmy et al., 2023) and EAP (Syed et al., 2024); and (2) gradient-masking-based algorithms, including weight pruning (WP) methods (Louizos et al., 2018; Cao et al., 2021; Sanh et al., 2020; De Cao et al., 2022), an edge pruning (EP) method (Bhaskar et al., 2024), and our novel joint pruning method. See Appendix C for details about our reproduction of these.

**LM Selection:** We compare to other methods using GPT-2 base (small) model, as it is the only model supported by the original implementation of every method.

## 5 Experiment Results

Table 2 shows the results of DiscoGP compared to the baseline methods. Due to page limits, full results for the OQA task are shown in Appendix D; the breakdown supports the same findings. For each experiment, we run the sheaf-discovery method five times and report average performance. GPT-2 achieves near-perfect performance on all BLiMP and IOI tasks, so we conduct our experiments on the full datasets. GPT-2 performs worse on the OQA PARAREL tasks, on the other hand, so we run experiments only on data samples where the original model answers the question correctly, discarding prompts where it fails, as it is unclear whether searching for a sheaf over a function the LM does not mimic would yield meaningful results.

Overall, we find that DiscoGP outperforms all of the baseline discovery methods. It achieves the highest functional fidelity — measured either as task accuracy or as KL divergence — compared to other baselines while using the fewest weight parameters or computation edges.

Method	Sheaf Acc. (%)	KL Div Acc. (%)	Comp. Acc. (%)	Weight Density (%)	Edge Density (%)
DiscoGP-MA	100	0.014	45.8	2.14	2.49
ACDC-MA	51.6	0.120	41.4	100	2.45

Table 3: When mean ablation (MA) is applied, DiscoGP shows the same kind of performance advantage compared to ACDC.

That said, our method is applicable to other ablation types such as mean ablation, by setting the residual term to the averaged distribution when the mask is 0, instead of setting it to 0. Table 3 presents a comparison of DiscoGP-MA to ACDC-MA for the IOI task.

**Discussion: Greedy threshold-based methods may not be suitable for sheaf discovery.** Interestingly, we observe that the performance of greedy threshold-based methods (ACDC and EAP) is less stable across tasks and, for more complex tasks, especially the PARAREL tasks (Appendix D), these methods reach near-random performance when given the same sparsity budget as DiscoGP. It is possible that greedy threshold-based methods are simply not well suited to any kind of circuit discovery.

Nevertheless, we should take this opportunity to elaborate on the difference between sheaf discovery and other construals of automatic circuit discovery. First and foremost, the two tasks differ in their goals and motivations. Let us revisit the famous example studied by Wang et al. (2022): “**When Mary and John went to the store, John gave a drink to \_\_**”, where **Mary** is the correct answer and **John** is the incorrect one. Up to now, the automatic circuit-discovery task has aimed to identify all the important computation edges and components that, when perturbed, cause the greatest change to the final output, potentially steering the model away from responding **Mary** to **John**. Our results show that simply taking the collection of these important components does not always yield a self-contained mechanism that can perform the task in isolation. Sheaf discovery, on the other hand, aims to capture and identify such a self-contained mechanism (the sheaf).

ACDC and EAP should use ablation and they do: both include *mean ablation*, which sets the activation to the average output across a reference distribution obtained by running a sample dataset through the model; and *interchange ablation*, which replaces the activation with its value

Task	Clean-Ablated Edge similarity		
	Mean	Interchange	Random
Agreement	0.878	0.907	0.582
IOI	0.943	0.996	0.597
OQA PARAREL	0.951	0.960	0.556

Table 4: Average cosine similarity between clean and corrupted ablated edge representations across three datasets. Mean and interchange ablations do not substantially affect the models’ overall performance.

Task	Evaluation Tasks					
	AGA	ANA	DNA	DNA i	DNA a	DNA ai
AGA	-	98.0	99.7	99.7	91.9	94.8
ANA	94.0	-	99.7	100	91.9	92.0
DNA	92.3	86.3	-	93.0	90.3	91.2
DNA i	91.3	80.3	93.7	-	94.4	93.1
DNA a	93.0	94.6	94.2	90.5	-	94.9
DNA ia	91.7	90.1	92.3	94.5	94.2	-
Orig.	99.0	100	94.7	95.3	96.0	95.7

Table 5: Composing sheaves largely preserves functional performance. Each entry shows the performance (accuracy in %) of a composed circuit (row + column) evaluated on the task associated with the column. For example, the value in column AGA, row ANA shows the performance of the composed circuit (ANA + AGA) on the AGA task. Original (non-composed) sheaf performance is listed in the final row for reference.

from corrupted input, created by modifying specific input tokens. These two ablation methods are not suitable for sheaf discovery, as mean-ablated and interchange-ablated components may still retain a large amount of task-related information (Table 4). This observation is supported by recent work (Adolfi et al., 2025; Shi et al., 2024) showing that these ablation- and patching-based methods may not achieve optimal functional fidelity.

## 6 Analysis and Findings

**Finding 1: Sheaves identified by DiscoGP can be composed while preserving functionality.** We find that *functional composition of sheaves* is possible under the DiscoGP framework. That is, suppose we have two sheaves that perform tasks A and B, respectively. Simply composing their masks,  $m = m_A \cup m_B$ , can yield a new sheaf that performs both tasks with largely the same performance. Table 5 shows the performance of such compositions across different BLiMP paradigms.

Overall, we observe good composition performance, with the composed sheaves’ accuracies reaching 80-100% across all BLiMP paradigms. To the best of our knowledge, our result is the first

Sheaf 1	Sheaf 2	Edge Overlap	Weight Overlap
AGA	DNA	14.86% (251)	2.69% (8020)
ANA	DNA	16.19% (277)	1.12% (14816)
ANA	AGA	18.32% (266)	0.91% (17693)
DNA	DNA irr	21.07% (317)	4.72% (69364)
DNA	DNA adj	18.46% (332)	4.96% (74782)
DNA	DNA irr adj	18.24% (323)	6.06% (96727)

Table 6: Sheaf overlap across different BLiMP tasks. The results indicate a trend where similar tasks exhibit higher sheaf overlaps. The overlap percentages are followed by the exact number of overlaps in brackets.

successful sheaf or circuit composition in the wild. Mondorf et al. (2025) studied circuit composition, but their experiments were limited to synthetic toy models generated using Tracr (Lindner et al., 2023). Composition would be important for demonstrating the practical utility of sheaves because it means that primitive sheaves can be combined to perform multiple, or possibly more complex tasks without having to re-discover every possible combination.

This suggests that at least some degree of modularity is salvageable from LMs after pre-training, although clearly more experimentation is necessary. We hope this finding will motivate future work on modularity and sheaf composition.

**Finding 2: Sheaf similarity reflects functional similarity.** Table 6 illustrates the overlap levels between different sheaves. The overlap percentages are calculated by dividing the number of overlap cases by the size of the logical union of the two masks. In this analysis, we only considered the agreement tasks as their task similarity is easier to perceive. BLiMP offers several variants of the DNA paradigms, and we observe here a relatively high level of sheaf overlap in terms of both weights and edges. ANA and AGA, on the other hand, exhibit greater similarity to each other than to DNA as paradigms, because ANA and AGA follow similar sentence templates (see Appendix B). This similarity between ANA and AGA is reflected in the degree of edge overlap, but not in weight overlap. We conjecture that this distinction between weight and edge overlap is due to the different roles they may play: weights store information, while edges guide the function of the task. While ANA and AGA share similar templates (and therefore exhibit higher edge overlap), performing the task requires distinct parametrized information (resulting in lower weight overlap).

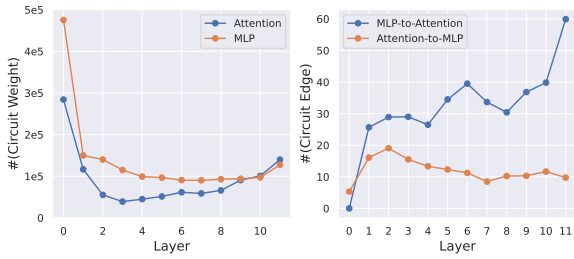


Figure 3: **Left:** Number of unmasked MLP and attention weights at each layer of the capital city OQA sheaf. **Right:** Number of edges ending at each layer from preceding MLPs to current-layer attention heads and from preceding attention heads to current-layer MLPs.

**Finding 3: Unveiling the factual recall pipeline in GPT.** Lastly, we find some confirmation of the *factual recall pipeline* hypothesis, namely that recall occurs in two distinct stages (Meng et al., 2022; Geva et al., 2023; Niu et al., 2024; Hernandez et al., 2024). The left panel of Figure 3 illustrates the layer-wise average number of MLP and attention weight parameters retained in the 12 relation-specific DiscoGP sheaves learned from PARAREL. We observe that MLPs retain substantially more weights in the OQA sheaves compared to attention heads, especially in the lower transformer layers. This finding aligns with recent work that has observed that MLP sublayers function as key-value memory for factual knowledge *extraction* (Geva et al., 2022). Conversely, the right panel of Figure 3 shows the number of sheaf edges at each layer, detailing connections from lower-layer attention heads to current-layer MLPs (Attention to MLP) and from preceding MLPs to current-layer attention heads (MLP to Attention). Notably, the set of connections in upper layers is dominated by MLP-to-attention edges. This observation supports recent findings in mechanistic interpretability suggesting that attention heads play a major role in *propagating* the retrieved factual knowledge from early-site MLPs to upper transformer layers, thereby selecting the most relevant information for answering questions (Geva et al., 2023).

## 7 Conclusion

In this work, we have proposed the notion of a sheaf, and a novel means of discovering them, DiscoGP. The sheaves discovered by DiscoGP have high functional fidelity using few connections and edges, by combining weight and edge pruning. This method operates with neuron-level granularity and reveals several novel insights into the internal

workings of LMs (sheaf modularity and overlap), while also confirming a previously observed trend (the factual recall pipeline).

## Acknowledgement

We thank the anonymous reviewers and the area chair for their insightful and constructive feedback.

## Limitations

While our experimental setup is sufficiently comprehensive for the purposes of this study, there is always room to expand the range of tasks and language models evaluated. We focus on GPT-2 to enable direct comparisons with other publicly available systems, but future work could consider larger or more recent models. Additionally, our experiments are limited to English, and extending the analysis to other languages would help assess the generality of our findings.

## References

Federico Adolfi, Martina G. Vilas, and Todd Wareham. 2025. The Computational Complexity of Circuit Discovery for Inner Interpretability. In *The Thirteenth International Conference on Learning Representations*.

Deniz Bayazit, Negar Foroutan, Zeming Chen, Gail Weiss, and Antoine Bosselut. 2023. *Discovering Knowledge-Critical Subnetworks in Pretrained Language Models*. *Preprint*, arXiv:2310.03084.

Yoshua Bengio, Nicholas Léonard, and Aaron Courville. 2013. *Estimating or Propagating Gradients Through Stochastic Neurons for Conditional Computation*. *Preprint*, arXiv:1308.3432.

Adithya Bhaskar, Alexander Wettig, Dan Friedman, and Danqi Chen. 2024. Finding Transformer Circuits With Edge Pruning. In *The Thirty-eighth Annual Conference on Neural Information Processing Systems*.

Steven Cao, Victor Sanh, and Alexander Rush. 2021. *Low-Complexity Probing via Finding Subnetworks*. In *Proceedings of the 2021 Conference of the North American Chapter of the Association for Computational Linguistics: Human Language Technologies*, pages 960–966, Online. Association for Computational Linguistics.

Arthur Conmy, Augustine N. Mavor-Parker, Aengus Lynch, Stefan Heimersheim, and Adrià Garriga-Alonso. 2023. Towards Automated Circuit Discovery for Mechanistic Interpretability. In *Thirty-Seventh Conference on Neural Information Processing Systems*.

Róbert Csordás, Sjoerd van Steenkiste, and Jürgen Schmidhuber. 2021. Are Neural Nets Modular? Inspecting Functional Modularity Through Differentiable Weight Masks. In *International Conference on Learning Representations*.

Damai Dai, Li Dong, Yaru Hao, Zhifang Sui, Baobao Chang, and Furu Wei. 2022. [Knowledge Neurons in Pretrained Transformers](#). In *Proceedings of the 60th Annual Meeting of the Association for Computational Linguistics (Volume 1: Long Papers)*, pages 8493–8502, Dublin, Ireland. Association for Computational Linguistics.

Nicola De Cao, Leon Schmid, Dieuwke Hupkes, and Ivan Titov. 2022. [Sparse Interventions in Language Models with Differentiable Masking](#). In *Proceedings of the Fifth BlackboxNLP Workshop on Analyzing and Interpreting Neural Networks for NLP*, pages 16–27, Abu Dhabi, United Arab Emirates (Hybrid). Association for Computational Linguistics.

Jacob Devlin, Ming-Wei Chang, Kenton Lee, and Kristina Toutanova. 2019. [BERT: Pre-training of Deep Bidirectional Transformers for Language Understanding](#). In *Proceedings of the 2019 Conference of the North American Chapter of the Association for Computational Linguistics: Human Language Technologies, Volume 1 (Long and Short Papers)*, pages 4171–4186, Minneapolis, Minnesota. Association for Computational Linguistics.

Yanai Elazar, Nora Kassner, Shauli Ravfogel, Abhijasha Ravichander, Eduard Hovy, Hinrich Schütze, and Yoav Goldberg. 2021. [Measuring and Improving Consistency in Pretrained Language Models](#). *Transactions of the Association for Computational Linguistics*, 9:1012–1031.

Nelson Elhage, Neel Nanda, Catherine Olsson, Tom Henighan, Nicholas Joseph, Ben Mann, Amanda Askell, Yuntao Bai, Anna Chen, Tom Conerly, Nova DasSarma, Dawn Drain, Deep Ganguli, Zac Hatfield-Dodds, Danny Hernandez, Andy Jones, Jackson Kernion, Liane Lovitt, Kamal Ndousse, and 6 others. 2021. A Mathematical Framework for Transformer Circuits. *Transformer Circuits Thread*.

Matthew Finlayson, Aaron Mueller, Sebastian Gehrmann, Stuart Shieber, Tal Linzen, and Yonatan Belinkov. 2021. [Causal Analysis of Syntactic Agreement Mechanisms in Neural Language Models](#). In *Proceedings of the 59th Annual Meeting of the Association for Computational Linguistics and the 11th International Joint Conference on Natural Language Processing (Volume 1: Long Papers)*, pages 1828–1843, Online. Association for Computational Linguistics.

Jonathan Frankle and Michael Carbin. 2019. The Lottery Ticket Hypothesis: Finding Sparse, Trainable Neural Networks. In *International Conference on Learning Representations*.

Atticus Geiger, Hanson Lu, Thomas Icard, and Christopher Potts. 2021. Causal Abstractions of Neural Networks. In *Advances in Neural Information Processing Systems*, volume 34, pages 9574–9586. Curran Associates, Inc.

Mor Geva, Jasmijn Bastings, Katja Filippova, and Amir Globerson. 2023. [Dissecting Recall of Factual Associations in Auto-Regressive Language Models](#). In *Proceedings of the 2023 Conference on Empirical Methods in Natural Language Processing*, pages 12216–12235, Singapore. Association for Computational Linguistics.

Mor Geva, Avi Caciularu, Kevin Wang, and Yoav Goldberg. 2022. [Transformer Feed-Forward Layers Build Predictions by Promoting Concepts in the Vocabulary Space](#). In *Proceedings of the 2022 Conference on Empirical Methods in Natural Language Processing*, pages 30–45, Abu Dhabi, United Arab Emirates. Association for Computational Linguistics.

Mor Geva, Roei Schuster, Jonathan Berant, and Omer Levy. 2021. [Transformer Feed-Forward Layers Are Key-Value Memories](#). In *Proceedings of the 2021 Conference on Empirical Methods in Natural Language Processing*, pages 5484–5495, Online and Punta Cana, Dominican Republic. Association for Computational Linguistics.

Nicholas Goldowsky-Dill, Chris MacLeod, Lucas Sato, and Aryaman Arora. 2023. [Localizing Model Behavior with Path Patching](#). *Preprint*, arXiv:2304.05969.

Demi Guo, Alexander Rush, and Yoon Kim. 2021. [Parameter-Efficient Transfer Learning with Diff Pruning](#). In *Proceedings of the 59th Annual Meeting of the Association for Computational Linguistics and the 11th International Joint Conference on Natural Language Processing (Volume 1: Long Papers)*, pages 4884–4896, Online. Association for Computational Linguistics.

Michael Hanna, Ollie Liu, and Alexandre Variengien. 2023. How Does GPT-2 Compute Greater-Than?: Interpreting Mathematical Abilities in a Pre-Trained Language Model. In *Thirty-Seventh Conference on Neural Information Processing Systems*.

Michael Hanna, Sandro Pezzelle, and Yonatan Belinkov. 2024. Have Faith in Faithfulness: Going Beyond Circuit Overlap When Finding Model Mechanisms. In *ICML 2024 Workshop on Mechanistic Interpretability*.

Evan Hernandez, Arnab Sen Sharma, Tal Haklay, Kevin Meng, Martin Wattenberg, Jacob Andreas, Yonatan Belinkov, and David Bau. 2024. Linearity of Relation Decoding in Transformer Language Models. In *The Twelfth International Conference on Learning Representations*.

Yihuai Hong, Lei Yu, Haiqin Yang, Shauli Ravfogel, and Mor Geva. 2024. [Intrinsic Evaluation of Unlearning Using Parametric Knowledge Traces](#). *Preprint*, arXiv:2406.11614.

Robert Huben, Hoagy Cunningham, Logan Riggs Smith, Aidan Ewart, and Lee Sharkey. 2024. Sparse Autoencoders Find Highly Interpretable Features in Language Models. In *The Twelfth International Conference on Learning Representations*.

Michael A. Lepori, Thomas Serre, and Ellie Pavlick. 2023. Break It Down: Evidence for Structural Compositionality in Neural Networks. In *Thirty-Seventh Conference on Neural Information Processing Systems*.

David Lindner, Janos Kramar, Sebastian Farquhar, Matthew Rahtz, Thomas McGrath, and Vladimir Mikulik. 2023. Tracr: Compiled transformers as a laboratory for interpretability. In *Thirty-Seventh Conference on Neural Information Processing Systems*.

Christos Louizos, Max Welling, and Diederik P. Kingma. 2018. Learning Sparse Neural Networks through L\_0 Regularization. In *International Conference on Learning Representations*.

Samuel Marks, Can Rager, Eric J. Michaud, Yonatan Belinkov, David Bau, and Aaron Mueller. 2024. Sparse Feature Circuits: Discovering and Editing Interpretable Causal Graphs in Language Models. In *The Thirteenth International Conference on Learning Representations*.

Kevin Meng, David Bau, Alex J. Andonian, and Yonatan Belinkov. 2022. Locating and Editing Factual Associations in GPT. In *Advances in Neural Information Processing Systems*.

Philipp Mondorf, Sondre Wold, and Barbara Plank. 2025. Circuit Compositions: Exploring Modular Structures in Transformer-Based Language Models. *Preprint*, arXiv:2410.01434.

Neel Nanda. 2022. A Comprehensive Mechanistic Interpretability Explainer & Glossary.

Neel Nanda. 2023. Attribution Patching: Activation Patching At Industrial Scale.

Neel Nanda and Joseph Bloom. 2022. Transformer-Lens.

Jingcheng Niu, Andrew Liu, Zining Zhu, and Gerald Penn. 2024. What does the Knowledge Neuron Thesis Have to do with Knowledge? In *The Twelfth International Conference on Learning Representations*.

Jingcheng Niu, Xingdi Yuan, Tong Wang, Hamidreza Saghir, and Amir H. Abdi. 2025. Llama See, Llama Do: A Mechanistic Perspective on Contextual Entainment and Distraction in LLMs. In *Proceedings of the 63rd Annual Meeting of the Association for Computational Linguistics (Volume 1: Long Papers)*, pages 16218–16239, Vienna, Austria. Association for Computational Linguistics.

Chris Olah, Nick Cammarata, Ludwig Schubert, Gabriel Goh, Michael Petrov, and Shan Carter. 2020. *Zoom In: An Introduction to Circuits*. *Distill*, 5(3):10.23915/distill.00024.001.

OpenAI. 2023. GPT-4 Technical Report. *Preprint*, arXiv:2303.08774.

Alec Radford, Jeffrey Wu, Rewon Child, David Luan, Dario Amodei, and Ilya Sutskever. 2019. Language Models are Unsupervised Multitask Learners. *OpenAI Blog*, page 24.

Colin Raffel, Noam Shazeer, Adam Roberts, Katherine Lee, Sharan Narang, Michael Matena, Yanqi Zhou, Wei Li, and Peter J. Liu. 2020. Exploring the Limits of Transfer Learning with a Unified Text-to-Text Transformer. *Preprint*, arXiv:1910.10683.

Victor Sanh, Lysandre Debut, Julien Chaumond, and Thomas Wolf. 2020. DistilBERT, a distilled version of BERT: Smaller, faster, cheaper and lighter. *Preprint*, arXiv:1910.01108.

Pedro Savarese, Hugo Silva, and Michael Maire. 2020. Winning the Lottery with Continuous Sparsification. In *Advances in Neural Information Processing Systems*, volume 33, pages 11380–11390. Curran Associates, Inc.

Claudia Shi, Nicolas Beltran-Velez, Achille Nazaret, Carolina Zheng, Adrià Garriga-Alonso, Andrew Jesson, Maggie Makar, and David Blei. 2024. Hypothesis Testing the Circuit Hypothesis in LLMs. In *ICML 2024 Workshop on Mechanistic Interpretability*.

Aaquib Syed, Can Rager, and Arthur Conmy. 2024. Attribution Patching Outperforms Automated Circuit Discovery. In *Proceedings of the 7th BlackboxNLP Workshop: Analyzing and Interpreting Neural Networks for NLP*, pages 407–416, Miami, Florida, US. Association for Computational Linguistics.

Hugo Touvron, Louis Martin, Kevin Stone, Peter Albert, Amjad Almahairi, Yasmine Babaei, Nikolay Bashlykov, Soumya Batra, Prajjwal Bhargava, Shruti Bhosale, Dan Bikel, Lukas Blecher, Cristian Canton Ferrer, Moya Chen, Guillem Cucurull, David Esibou, Jude Fernandes, Jeremy Fu, Wenjin Fu, and 49 others. 2023. Llama 2: Open Foundation and Fine-Tuned Chat Models. *Preprint*, arXiv:2307.09288.

Ashish Vaswani, Noam Shazeer, Niki Parmar, Jakob Uszkoreit, Llion Jones, Aidan N Gomez, Łukasz Kaiser, and Illia Polosukhin. 2017. Attention is All you Need. In *Advances in Neural Information Processing Systems*, volume 30. Curran Associates, Inc.

Jesse Vig, Sebastian Gehrmann, Yonatan Belinkov, Sharon Qian, Daniel Nevo, Yaron Singer, and Stuart Shieber. 2020. Investigating Gender Bias in Language Models Using Causal Mediation Analysis. In *Advances in Neural Information Processing Systems*, volume 33, pages 12388–12401. Curran Associates, Inc.

Kevin Ro Wang, Alexandre Variengien, Arthur Conmy, Buck Shlegeris, and Jacob Steinhardt. 2022. Interpretability in the Wild: A Circuit for Indirect Object Identification in GPT-2 Small. In *The Eleventh International Conference on Learning Representations*.

Alex Warstadt, Alicia Parrish, Haokun Liu, Anhad Mo-hananey, Wei Peng, Sheng-Fu Wang, and Samuel R. Bowman. 2020. **BLiMP: The Benchmark of Linguistic Minimal Pairs for English**. *Transactions of the Association for Computational Linguistics*, 8:377–392.

Zhengxuan Wu, Atticus Geiger, Thomas Icard, Christopher Potts, and Noah Goodman. 2023. Interpretability at Scale: Identifying Causal Mechanisms in Alpaca. In *Thirty-Seventh Conference on Neural Information Processing Systems*.

Lei Yu, Meng Cao, Jackie CK Cheung, and Yue Dong. 2024a. **Mechanistic Understanding and Mitigation of Language Model Non-Factual Hallucinations**. In *Findings of the Association for Computational Linguistics: EMNLP 2024*, pages 7943–7956, Miami, Florida, USA. Association for Computational Linguistics.

Lei Yu, Virginie Do, Karen Hambardzumyan, and Nicola Cancedda. 2024b. Robust LLM Safeguarding via Refusal Feature Adversarial Training. In *The Thirteenth International Conference on Learning Representations*.

Dinghuai Zhang, Kartik Ahuja, Yilun Xu, Yisen Wang, and Aaron Courville. 2021. Can Subnetwork Structure be the Key to Out-of-Distribution Generalization? In *Proceedings of the 38th International Conference on Machine Learning*, volume 139 of *Proceedings of Machine Learning Research*, pages 12356–12367. PMLR.

Fred Zhang and Neel Nanda. 2023. Towards Best Practices of Activation Patching in Language Models: Metrics and Methods. In *The Twelfth International Conference on Learning Representations*.

Lin Zhang, Wenshuo Dong, Zhuoran Zhang, Shu Yang, Lijie Hu, Ninghao Liu, Pan Zhou, and Di Wang. 2025. **EAP-GP: Mitigating Saturation Effect in Gradient-based Automated Circuit Identification**. *Preprint*, arXiv:2502.06852.

## A DiscoGP Implementation Details

**Post-hoc Sheaf Pruning** Since the training objective (8) does not consider graph connectivity, we can further simplify the model by (1) removing a node  $v$  from the computation graph if all of its weights have been pruned, and (2) performing a reverse BFS from the output node to eliminate edges that do not contribute to the final result.

**Split QKV Pruning** Following Conmy et al. (2023), we separate the query (Q), key (K) and value (V) activations and introduce an “output” node within each attention head. Figure 4 shows an illustration of the configuration.

## B Evaluation Tasks & Data

**BLiMP** BLiMP (Warstadt et al., 2020) consists of 67 individual datasets, each containing minimally different sentence pairs that contrast in grammatical acceptability and isolate specific phenomena in syntax, morphology, or semantics. However, BLiMP was designed for bidirectional LMs such as BERT, which require the model to attend to both preceding and following context. Therefore, we use the six BLiMP paradigms applicable to decoder-only LMs (specifically GPT-2). See Table 7 for example contrasting sentence pairs and their corresponding query prompts for circuit discovery.

**Indirect object identification** Wang et al. (2022) created dataset samples for IOI using templates with random single-token names, places and items. We follow their data curation pipeline by taking the same set of 15 templates and candidate-infilling words to generate our sheaf-discovery dataset. At each trial, we randomly draw a template and a set of infilling tokens to construct a full sentence. We then convert the generated sentence into a binary classification question, where the input prompt is the sentence prefix without the last indirect object, and the two candidates for next token are the indirect object and the subject tokens. See Table 8 and 9 for a complete list of IOI sentence templates and candidate-infilling words.

**PARAREL** We use the PARAREL dataset by Elazar et al. (2021), which consists of 38 relation types and 27,738 (subject, relation, object) fact triples such as (*Canada*, capital city, *Ottawa*). We then use the templates created by (Dai et al.,

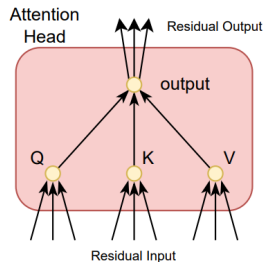


Figure 4: Split QKV Pruning.

Agreement Phenomenon	Good sentence	Bad sentence	Converted input query	True answer	False answer
Anaphor Gender Agreement	Katherine can't help herself.	Katherine can't help himself.	Katherine can't help	herself	himself
Anaphor Number Agreement	Susan revealed herself.	Susan revealed themselves.	Susan revealed	herself	themselves
Det Noun Agr. 1	Raymond is selling this sketch.	Raymond is selling this sketches.	Raymond is selling this	sketch	sketches
Det Noun Agr. Irr. 1	Laurie hasn't lifted those cacti.	Laurie hasn't lifted those cactus.	Laurie hasn't lifted those	cacti	cactus
Det Noun Agr. with Adj. 1	Rebecca was criticizing those good documentaries.	Rebecca was criticizing those good documentary.	Rebecca was criticizing those good	documentaries	documentary
Det Noun Agr. with Adj. Irr. 1	Some waiters broke this lost foot.	Some waiters broke this lost feet.	Some waiters broke this lost	foot	feet

Table 7: Examples of the BLiMP and their converted data.

Templates
Then, [B] and [A] went to the [PLACE]. [B] gave a [OBJECT] to [A]
Then, [B] and [A] had a lot of fun at the [PLACE]. [B] gave a [OBJECT] to [A]
Then, [B] and [A] were working at the [PLACE]. [B] decided to give a [OBJECT] to [A]
Then, [B] and [A] were thinking about going to the [PLACE]. [B] wanted to give a [OBJECT] to [A]
Then, [B] and [A] had a long argument, and afterwards [B] said to [A]
After [B] and [A] went to the [PLACE], [B] gave a [OBJECT] to [A]
When [B] and [A] got a [OBJECT] at the [PLACE], [B] decided to give it to [A]
When [B] and [A] got a [OBJECT] at the [PLACE], [B] decided to give the [OBJECT] to [A]
While [B] and [A] were working at the [PLACE], [B] gave a [OBJECT] to [A]
While [B] and [A] were commuting to the [PLACE], [B] gave a [OBJECT] to [A]
After the lunch, [B] and [A] went to the [PLACE]. [B] gave a [OBJECT] to [A]
Afterwards, [B] and [A] went to the [PLACE]. [B] gave a [OBJECT] to [A]
Then, [B] and [A] had a long argument. Afterwards [B] said to [A]
The [PLACE] [B] and [A] went to had a [OBJECT]. [B] gave it to [A]
Friends [B] and [A] found a [OBJECT] at the [PLACE]. [B] gave it to [A]

Table 8: Sentence templates for generating the IOI dataset.

Placeholder Type	Candidate Infilling Words
[A] and [B] (names)	Michael, Christopher, Jessica, Matthew, Ashley, Jennifer, Joshua, Daniel, David, James, Robert, John, Joseph, Andrew, Ryan, Bran Justin, Sarah, William, Jonathan, Stephanie, Brian, Nicole, Nicho Heather, Eric, Elizabeth, Adam, Megan, Melissa, Kevin, Steven, Timothy, Christina, Kyle, Rachel, Laura, Lauren, Amber, Brittan Richard, Kimberly, Jeffrey, Amy, Crystal, Michelle, Tiffany, Jere Mark, Emily, Aaron, Charles, Rebecca, Jacob, Stephen, Patrick, Kelly, Samantha, Nathan, Sara, Dustin, Paul, Angela, Tyler, Scot Andrea, Gregory, Erica, Mary, Travis, Lisa, Kenneth, Bryan, Lin Jose, Alexander, Jesse, Katie, Lindsay, Shannon, Vanessa, Court Alicia, Cody, Allison, Bradley, Samuel.
[PLACE]	store, garden, restaurant, school, hospital, office, house, station.
[OBJECT]	ring, kiss, bone, basketball, computer, necklace, drink, snack.

Table 9: Candidate infilling words of IOI sentence templates.

Relation ID	Relation	No. of Queries	Sample Query	True answer
P103	native language	977	The mother tongue of Victor Horta is	Dutch
P138	named after	645	Rawlings Gold Glove Award, which is named for	glove
P159	headquarters location	967	The headquarter of Strait Shipping is located in	Wellington
P176	manufacturer	982	Honda RA272 is produced by	Honda
P264	record label	429	Johnny Carroll’s record label is	Decca
P279	subclass of	964	Nucleoprotein 62, a type of	protein
P30	continent	975	Romulus Glacier is located in	Antarctica
P407	language of work or name	877	Ten Years Gone is a work written in	English
P449	original network	881	Himalaya with Michael Palin was originally aired on	BBC
P495	country of origin	909	Mundo Obrero was from	Spain
P1376	capital of	234	Guangzhou is the capital of	Guangdong
P36	capital	703	The capital city of Porto District is	Porto

Table 10: PARAREL relations and sample queries used for circuit discovery.

2022) to convert each fact triple into multiple query prompts (e.g. “**The capital city of Canada is \_\_**”). We take prompts generated from triples with 12 out of 38 PARAREL relations that satisfy the following two conditions: 1) there is a unique object entity answer for each (subject, relation) pair; and 2) the object word always comes at the end of the template-generated sentence so that it can be predicted by an autoregressive language model. We finally obtained a total of 9,543 queries as our dataset of open-domain question answering, and we learn a circuit for each relational dataset for every circuit-discovery method. See Table 10 for a list of the 12 relations we used together with the example fact triples and queries.

## C Baseline Methods

For the greedy, threshold-based approaches, we obtain the original implementations released by the authors and adapt them to work with the same task and configurations as DiscoGP.<sup>3</sup> Bhaskar et al. (2024) have released their implementation online,<sup>4</sup> which is equivalent to our edge pruning setting, where no weight pruning is applied.

For the threshold-based greedy search algorithms, since performance is not an objective in the circuit-discovery process, we can obtain circuits with any level of sparsity by adjusting the thresholds. Therefore, we tune the threshold  $\tau$  for each task and report the result that has a comparable — and larger — sparsity budget than DiscoGP. This puts ACDC and EAP at an advantage compared to DiscoGP in the sparsity–performance trade-off,

yet our results show that DiscoGP still outperforms both.

## D Detailed PARAREL Results

Table 11 and 12 list our PARAREL results. Again, DiscoGP achieves the best performance across all tasks while mostly using the fewest weight parameters and edges. The PARAREL task differs from the BLiMP and IOI tasks in that test set and training set performance diverge significantly. This is expected, as factual information tends to be more dispersed. For example, Dai et al. (2022); Niu et al. (2024) found that each piece of factual information (e.g., Canada’s capital is Ottawa) can be attributed to a handful of neurons, while Niu et al. (2024) found that the entire determiner–noun agreement can be attributed to the same amount of neurons.

<sup>3</sup>ACDC: <https://github.com/ArthurConmy/Automatic-Circuit-Discovery/> and EAP <https://github.com/Aaquib111/edge-attribution-patching>.

<sup>4</sup><https://github.com/princeton-nlp/Edge-Pruning>

Task	Discovery Method	Test Set Acc. (%) (higher is better)	Train Set Acc. (%) (higher is better)	KL Div. (lower is better)	Comp. Acc. (%) (random* is better)	Weight Density (%) (lower is better)	Edge Density (%) (lower is better)
P30	ACDC	0.30	0.27	0.3194	1.20	100	4.57
	EAP	1.18	1.63	0.3900	0.08	100	6.42
	Edge	92.1	89.5	0.0115	0.90	100	<b>2.34</b>
	Weight	86.8	92.6	0.0093	0.23	3.86	100
	DiscoGP	<b>95.6</b>	<b>92.6</b>	<b>0.0076</b>	0.35	<b>3.64</b>	3.01
P36	ACDC	0.72	0.86	0.3706	0.42	100	5.99
	EAP	1.18	1.86	0.3272	1.21	100	4.59
	Edge	62.7	90.5	0.0164	0.86	100	3.45
	Weight	67.3	90.3	0.0191	1.04	4.54	100
	DiscoGP	<b>69.2</b>	<b>91.1</b>	<b>0.0094</b>	0.85	<b>4.17</b>	<b>3.22</b>
P103	ACDC	0.54	1.16	0.2913	0.36	100	5.18
	EAP	0.93	0.57	0.3329	0.51	100	5.32
	Edge	91.4	88.1	0.0345	0.88	100	2.02
	Weight	83.0	87.4	0.0231	0.96	<b>4.35</b>	100
	DiscoGP	<b>93.5</b>	<b>89.7</b>	<b>0.0202</b>	0.15	4.7	<b>3.36</b>
P138	ACDC	0.96	0.59	0.3096	1.29	100	4.99
	EAP	1.98	0.78	0.2429	0.31	100	5.40
	Edge	64.9	96	0.022	1.52	100	2.33
	Weight	63.3	92.4	0.0375	0.73	1.57	100
	DiscoGP	<b>68.0</b>	<b>94.9</b>	<b>0.029</b>	0.46	<b>1.34</b>	<b>1.9</b>
P159	ACDC	0.56	1.64	0.3630	0.35	100	4.92
	EAP	1.78	1.44	0.3011	0.30	100	6.41
	Edge	57.3	84.2	0.0552	0.91	100	<b>2.05</b>
	Weight	58.8	88.7	0.0276	0.59	3.38	100
	DiscoGP	<b>62.5</b>	<b>89.8</b>	0.0168	0.57	<b>3.79</b>	2.81
P176	ACDC	0.53	1.77	0.3823	0.48	100	6.99
	EAP	0.91	1.39	0.3050	1.26	100	4.89
	Edge	86.5	98.6	0.0117	0.47	100	3.04
	Weight	86.0	99.2	<b>0.0095</b>	0.88	1.34	100
	DiscoGP	<b>95.6</b>	<b>99.4</b>	0.0104	0.85	<b>1.01</b>	<b>2.73</b>
P264	ACDC	1.51	0.51	0.2250	0.57	100	4.48
	EAP	0.27	0.39	0.2165	1.26	100	6.24
	Edge	77.3	89.4	0.0297	0.16	100	2.45
	Weight	82.3	90.8	0.0266	1.24	3.58	100
	DiscoGP	<b>82.9</b>	<b>90.3</b>	<b>0.0245</b>	0.77	<b>3.36</b>	<b>2.43</b>
P279	ACDC	1.30	0.54	0.3590	0.77	100	4.69
	EAP	0.74	0.55	0.3153	0.52	100	6.34
	Edge	69.5	87.0	0.0562	0.68	100	4.98
	Weight	75.5	93.9	0.0337	0.13	2.53	100
	DiscoGP	<b>76.9</b>	<b>95.2</b>	<b>0.0200</b>	0.47	<b>2.14</b>	<b>3.57</b>
P407	ACDC	1.41	1.51	0.3492	0.32	100	4.96
	EAP	0.49	0.66	0.2036	0.03	100	5.78
	Edge	80.1	93.9	0.0085	0.55	100	<b>2.1</b>
	Weight	77.0	94.1	0.0097	0.29	<b>1.94</b>	100
	DiscoGP	<b>83.3</b>	<b>95.0</b>	<b>0.0073</b>	0.97	2.24	2.89

Table 11: Sheaf-Discovery Performance Comparison across PARAREL relations. Again, DiscoGP achieves the best performance across all tasks while mostly using the fewest weight parameters and edges. The best-performing methods are highlighted in **bold**. \*: For complement sheaf accuracy, successful searches are expected to yield random performance. Therefore, scores in the vicinity of random indicate good performance, and direct comparison of complement scores is not meaningful. Table continues in Table 12.

Task	Discovery Method	Test Set Acc. (%) (higher is better)	Train Set Acc. (%) (higher is better)	KL Div. (lower is better)	Comp. Acc. (%) (random* is better)	Weight Density (%) (lower is better)	Edge Density (%) (lower is better)
P449	ACDC	0.59	1.20	0.5230	0.20	100	6.88
	EAP	0.87	0.33	0.4976	0.82	100	6.87
	Edge	70.4	93.3	<b>0.0090</b>	0.95	100	<b>3.36</b>
	Weight	71.4	93.7	0.0098	1.39	2.7	100
	DiscoGP	<b>74.7</b>	<b>93.7</b>	0.0099	1.09	<b>2.58</b>	3.43
P495	ACDC	0.22	0.22	0.5130	0.21	100	4.37
	EAP	1.30	0.47	0.4058	0.43	100	6.12
	Edge	65.8	86.1	0.115	0.76	100	3.92
	Weight	65.4	87.1	0.102	0.70	2.54	100
	DiscoGP	<b>70.7</b>	<b>90.3</b>	<b>0.082</b>	0.63	<b>2.08</b>	<b>2.17</b>
P1376	ACDC	1.22	1.76	0.5535	0.65	100	6.14
	EAP	0.38	0.76	0.5551	0.40	100	6.66
	Edge	49.4	89.3	0.101	0.77	100	3.57
	Weight	55.2	92.5	0.082	0.24	<b>1.68</b>	100
	DiscoGP	<b>57.7</b>	<b>94.6</b>	<b>0.047</b>	0.28	2.13	<b>3.36</b>

Table 12: Sheaf-Discovery Performance Comparison across PARAREL relations (Part 2).